Analysis of the Contention Access Period of IEEE 802.15.4 MAC

Iyappan Ramachandran Arindam K. Das, Sumit Roy
{iyappan,arindam,roy}@ee.washington.edu

Dept of EE, University of Washington
Seattle WA, 98195-2500

UWEE Technical Report
Number UWEETR-2006-0003
February 2006

Department of Electrical Engineering
University of Washington
Box 352500
Seattle, Washington 98195-2500
PHN: (206) 543-2150
FAX: (206) 543-3842
URL: http://www.ee.washington.edu

Analysis of the Contention Access Period of IEEE 802.15.4 MAC

Iyappan Ramachandran Arindam K. Das, Sumit Roy
{iyappan,arindam,roy}@ee.washington.edu

Dept of EE, University of Washington
Seattle WA, 98195-2500

University of Washington, Dept. of EE, UWEETR-2006-0003

February 2006

Abstract

The recent ratification of IEEE 802.15.4 PHY-MAC specifications for low-rate wireless personal area networks represents a significant milestone in promoting deployment of wireless sensor networks (WSNs) for a variety of commercial uses. The 15.4 specifications specifically target wireless networking among *low rate, low power and low cost* devices that is expected to be a key market segment for a large number of WSN applications. In this paper, we first analyze the performance of the contention access period specified in IEEE 802.15.4 standard, in terms of throughput and energy consumption. This analysis is facilitated by a modeling of the contention access period as *non-persistent CSMA with backoff*. We show that in certain applications, in which having an inactive period in the superframe may not be desirable due to delay constraints, shutting down the radio between transmissions provides significant savings in power without significantly compromising the throughput. We also propose and analyze the performance of a modification to the specification which could be used for applications in which MAC-level acknowledgements are not used. Extensive *ns*-2 simulations are used to verify the analysis.

1 Introduction

Wireless sensor networks (WSNs) are envisioned for a wide range of applications ranging from environmental surveillance, inventory tracking, health monitoring, home automation [9] [7] to networking in or around a human body. These networks, known as wireless body area networks (WBANs), are expected to enable medical sensing and/or wearable computing [14]. For many of these diverse applications, the sensor networks will share some common characteristics. For example, they may be ad-hoc, self configuring and requiring virtually no maintenance. Further, the sensors are expected to be inexpensive and deployment would typically be large-scale with enough built-in redundancy for adequate coverage of the sensing field. Since the nodes will be powered by small batteries, the radio itself and the protocol stack design must be energy conserving above all other considerations. The aggregate average throughput requirement for such monitoring applications is typically low, and could be a mix of real and non real-time traffic.

Much of the development in WSNs in recent years has focussed on new sensor node hardware - $i.e.$, integration of sensing and radio circuitry - as well as design of suitable networking protocols to meet the requirements of low cost and low power operation. Notable contributions in the design of sensor hardware have come from the PicoRadio project at UC, Berkeley [18] and the μAMPS project at MIT [22]. Examples of work in the area of protocol design include S-MAC from CENS at UCLA [26], WiseNET project at CSEM [11], etc. Companies like Crossbow Technologies, Sensoria Corp. and Ember Corp. have been making commercial hardware/software for WSNs.

Despite the above advances in both sensor hardware and development of suitable sensor networking protocols, the lack of a suitable WSN standard and associated commercial products has slowed the maturation process of this technology. The situation is expected to change with the release of the IEEE 802.15.4 Wireless MAC and PHY specifications for low-rate, low-power wireless personal area networks (WPANs) [13] due to significant interest from companies that are already beginning to ship products based on this standard. IEEE 802.15.4 based radio chips are available from Chipcon, Freescale Semiconductor and Ember Corp. Other examples of functional sensor device

offerings (motes) based on the IEEE 802.15.4 standard include Telos [17] and MICAz [8] from Crossbow Inc. and M2020 motes for Dust Networks' SmartMesh [10].

In spite of the large interest in the 802.15.4 standard, no adequate modeling of its behavior exists to date. The small body of literature is largely simulation based; [27] [28] developed an *ns*-2 based simulator and conducted several experiments to study aspects such as association, delay performance, collisions etc. In [16], the throughput and energy efficiency performances of 802.15.4 were assessed by simulations. The suitability of the standard for medical applications has been studied in [12] by means of OPNET simulations, while in [24] the authors have evaluated the performance of a wireless BAN of implanted devices using the 802.15.4 protocol. A basic analysis has been presented in [1] for the average power consumption without separate verification. To the best of our knowledge, our work is the first comprehensive analysis of key portions of the IEEE 802.15.4 MAC protocol.

We undertake a performance analysis of the contention access period (CAP) of the 802.15.4 superframe by modeling it as *non-persistent CSMA with backoff*. Non-persistent CSMA was first analyzed in [15] where the model presumed infinite nodes with an aggregate Poisson arrival of packets. Subsequently, [23] and [25] analyzed the throughput of non-persistent CSMA with a finite number of nodes by assuming that every node becomes ready to transmit independently in each slot with probability p, which is a protocol-dependent parameter. We extend the analysis to the case when the backoff characteristics at each node are as specified in IEEE 802.15.4. A Markov model is developed to determine the fractions of time that a node spends in different states, which are then used to determine the throughput and energy consumption characteristics. For this purpose, we use the transceiver characteristics of the commercially available CC2420 IEEE 802.15.4 radio [6]. We then suggest and analyze some modifications to the standard that could potentially improve the throughput and energy consumption of WSNs. We validate our proposed modification with extensive *ns*-2 simulations.

To summarize, the contributions of this paper are three-fold:

- We provide a comprehensive analysis of the throughput and energy efficiency of non-persistent CSMA when the back-off characteristics are known.
- We show that the IEEE 802.15.4 MAC can be accurately modeled as non-persistent CMSA with backoff. This is corroborated by means of *ns*-2 simulations.
- We propose and analyze a modification to the 802.15.4 standard that could result in significant improvements in throughput and energy efficiency in certain applications.

The rest of this paper is organized as follows. The next section gives a brief overview of the IEEE 802.15.4 standard specification. Model description and assumptions are provided in Section 3. Section 4 details the Markov chain modeling of the CAP as non-persistent CSMA with backoff. Throughput and energy consumption parameters are derived subsequently from the probabilities associated with the Markov chains. In Section 5, a modification to the contention mechanism is proposed and analyzed. Simulation results to validate our analysis of the standard and proposed modifications are provided in Section 6. Concluding remarks and pointers for future work are summarized in Section 7.

2 Overview of IEEE 802.15.4

A detailed description of the MAC and PHY characteristics of the IEEE 802.15.4 standard is available in [5]. The standard encompasses multiple frequency bands - one channel in the 868 MHz band with a data rate of 20 kbps, 10 channels in the 915 MHz band each with 40 kbps rate and 16 channels in the 2.4 GHz ISM band each supporting a data rate of 250 kbps. The 865 MHz and the 915 MHz radios employ direct-sequence spread spectrum with each data symbol being mapped onto a 15-chip PN sequence, followed by binary phase shift keying (BPSK) for chip modulation. The 2.4 GHz radio, on the other hand, maps each 4 bits of information onto a 32 chip PN sequence followed by offset orthogonal phase shift keying (O-QPSK). In this work, we confine ourselves to the 2.4 GHz radio since it is the only worldwide spectrum allocation, though our analysis can be extended straightforwardly to the other two bands by adjusting the channel characteristics accordingly.

Two topologies are supported by 802.15.4 - star and peer-to-peer - with the logical structure of the latter being defined by the network layer. Applications such as personal computer peripherals and WBANs would typically employ a one-hop star topology. Peer-to-peer topology allows for more complex formations like the cluster-tree and mesh networking topologies and may be the preferred choice for applications such as industrial and environmental

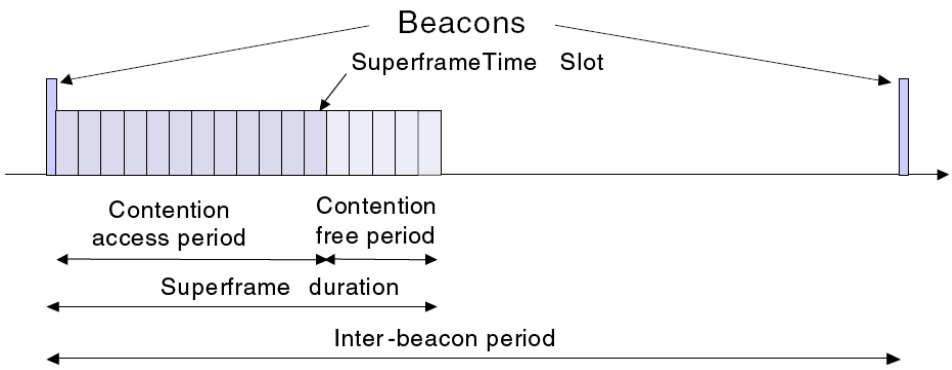

Figure 1: IEEE 802.15.4 superframe structure in beacon-enabled mode: reproduced from [1]

monitoring, inventory control, etc. An 802.15.4 network can work either in beacon-enabled or in non-beacon-enabled mode. In the former mode, communication is controlled by a network coordinator, which transmits regular beacons for synchronization and association procedures. In the non-beacon enabled mode, there are no regular beacons, but the coordinator may unicast beacons to a soliciting device. Communication among devices in the non-beacon-enabled mode uses unslotted CSMA for decentralized access.

A superframe structure is imposed in the beacon-enabled mode which begins with a beacon and is followed by an active and an optional inactive period as shown in Fig. 1. All communication takes place in the active period; in the inactive period, nodes are allowed to power down and conserve energy. The length of the superframe (called the beacon interval, BI) and the length of its active part (called the superframe duration, SD) are defined as follows:

$$\begin{aligned} BI &= aBaseSuperframeDuration \times 2^{\mathrm{BCO}} \\ SD &= aBaseSuperframeDuration \times 2^{\mathrm{SFO}} \end{aligned} \tag{1}$$

where $aBaseSuperframeDuration = 960$ symbols or 15.36 ms. The parameters BCO and SFO denote the beacon order and the superframe order respectively[1]. These values are determined by the coordinator and are restricted to be in the range $0 \leq SFO \leq BCO \leq 14$.

The active period of a superframe in turn may consist of a contention access period (CAP) and a contention free period (CFP). Channel access in the CAP is in the form of slotted-CSMA, while the coordinator allots guaranteed time slots (GTS) in the CFP for low latency applications. The slotted-CSMA algorithm works as follows. All nodes are synchronized and transmissions can begin only at the boundaries of time units called *backoff slots*. For simplicity, we will henceforth use the terms *backoff slots* and *slots* interchangeably. Each slot lasts 20 symbol durations (or 320 μs) and is denoted by t_{b_slot}. A node which has a packet ready for transmission first backs off for a random number of slots, chosen uniformly between 0 and $2^{BE} - 1$, before sensing the channel, where the parameter BE is the *backoff exponent* which is initially set to 3. This random backoff serves to reduce the probability of collisions among contending nodes. The channel sensing mechanism then ensures that the channel is clear of activity for a *contention window* (CW) duration, expressed in terms of number of backoff slots[2], before the node can attempt transmission. The 802.15.4 standard defines the CW duration to be of 2 backoff slots, or 640 μs. If the channel is found to be busy, the backoff exponent is incremented by one and a new number of slots is drawn for the node to wait, until the channel can be sensed again. This process is repeated until either BE equals the parameter $aMaxBE$ (which has a default value of 5), at which point it is frozen at $aMaxBE$, or, until a certain maximum number of permitted random backoff stages is reached, at which point an access failure is declared to the upper layer. The maximum number of permitted random backoff stages is determined by the parameter $macMaxCSMABackoffs$, which has a default value of 5.

[1]We denote the beacon and superframe orders with BCO and SFO instead of BO and SO as is done in the specifications, to differentiate from Backoff which we denote as BO.

[2]Note that the term *contention window* in 802.15.4 refers to the *fixed* number of slots that the channel has to be idle before a node can start to transmit, as opposed to a *random* number of slots in IEEE 802.11.

3 Model assumptions

In this work, we confine our evaluation to 802.15.4 networks operating in a one-hop star topology which would be preferred for applications such as WBANs where the coordinator is an externally worn device like a PDA or a cell phone, or a bedside monitoring station that collects data. Such star topologies may also exist inside clusters in larger networks of 802.15.4 devices. Since most of the unique features of the standard like coordinator assisted node synchronization, sleeping, *etc*. are in the beacon-enabled mode, we will only focus on this mode. We consider M nodes associated with a common coordinator in a one-hop star topology where all nodes are within carrier sensing range of each other. This ensures that an ongoing transmission will not be disrupted by other nodes.

Although having an inactive period allows the nodes to sleep periodically and conserve energy, it introduces undesirable delays in delay-critical monitoring applications like WBANs, particularly at higher beacon orders. Therefore, in our analysis, we assume that the entire superframe duration is active; $i.e.$, $SFO = BCO$ in (1). Since we are only concerned with MAC performance in the contention mode, the active period will be assumed not to have a contention free period. In a WSN which gathers information from the environment and forwards it to a base station (coordinator), most of the communication is *uplink* (nodes to coordinator), as opposed to *downlink* (coordinator to nodes). Consequently, we concentrate our analysis on the uplink mode only. This allows nodes to enter the sleep state depending on their own availability of data to transmit rather than having to stay awake for the entire active period.

Typically, wireless ad hoc networks and wireless LANs employ MAC level acknowledgements (ACKs) as a means to ensure reliable data transfer. In contrast, for dense wireless sensor networks, the required reliability can be provided by ensuring that there is sufficient redundancy in sensor deployment ($i.e.$, there is multiple overlapping sensor coverage for each region of interest). Since the coordinator is typically equipped with data aggregation capabilities, redundancy in sensor coverage obviates the need for acknowledging each packet. This is also beneficial from an energy consumption point of view, since a sensing node does not have to stay awake to receive the ACK after it has finished its data transmission. In this paper, therefore, we assume that MAC level acknowledgements are not employed. This assumption is also the basis for the modification we propose in Section 5.

Finally, packets are assumed to be of fixed N-slot duration and arrive at the nodes for transmission according to a Poisson arrival rate of λ packets per packet duration. Equivalently, the probability p that a node will get a packet to transmit at the next slot is $p = \lambda/N$. We do not consider any buffering at the nodes. This implies that new packets are not accepted for transmission ($p = 0$) when the node is currently transmitting, or, is attempting a transmission.

4 Analysis of the Contention Access Period (CAP)

In the following, we model the contention access period of IEEE 802.15.4 MAC as non-persistent CSMA with backoff. For the sake of tractability, we introduce certain approximations as discussed below. Simulation results discussed in Section 6 validate our assumptions. For notational clarity, all probabilities associated with channel states have a superscript 'c' ($e.g.$, p_i^c) and those associated with node states have a superscript 'n' ($e.g.$, p_i^n).

Approximation 1 The standard specifies that the nodes ensure that any transmission they initiate should be completed before the end of that beacon interval, $i.e.$, if nodes realize that a transmission cannot be finished within the beacon interval, it is postponed. We conjecture that this condition has negligible effect on the contention process and can be largely ignored, particularly for large values of the beacon order. Consequently, the contention access period can be analyzed simply as non-persistent CSMA.

Approximation 2 According to the non-persistent CSMA model, if a node senses the channel to be idle, it transmits its packet. Since computation of the probability that the channel is sensed idle in a given slot is difficult, we approximate it with the *steady state* probability that the channel is idle. Such an approximation has been used and shown to be satisfactory in [23] and [25]. Thus, every node sees a probability p_i^c that the channel is idle in the *first* of the two slots after every random backoff. We do *not* assume that channel idleness is independent from one sensing slot to the next. However, it is reasonable to assume channel state independence for two slots separated by a backoff duration, particularly when packet lengths are small. This approximation allows us to model a single node independently of all others.

Approximation 3 If the probability that an individual node begins transmission in any generic slot is known, the channel throughput and collision probability can be computed easily. However, computing the probability that any

node begins transmission *in any generic slot* is difficult. We therefore approximate this probability with the *steady-state* probability that a node transmits, p_t^n. The channel thus sees a probability p_t^n that an individual node begins transmission in any generic slot, except when it is already transmitting. This approximation effectively decouples the modeling of the channel states and the node states.

Approximation 4 The 802.15.4 standard specifies that the number of slots a node has to wait at each random backoff stage should be drawn from an uniform distribution. For the sake of analytical tractability, we replace the uniform distribution with a geometric distribution of the same mean, so that the backoff algorithm is memoryless. The transition out of the k^{th} random backoff stage is characterized by the parameter p_k^n, which is the probability that the node will attempt to sense the channel at the next slot. Such an approximation has been used in the analysis of IEEE 802.11 MAC (see [3] and [2]), with very accurate results.

4.1 Node state model

We model the behavior of an individual node by means of a Markov chain as shown in Fig. 2. A node is in IDLE state when it does not have a packet to transmit. When it receives a packet to transmit in a slot (with probability p), it transitions to the random backoff stage, BO_1, corresponding to the first backoff attempt. Since the backoff exponent $\text{BE} = 3$ for the first backoff BO_1, the number of slots that the node spends in BO_1 is a random variable drawn uniformly between 0 and $2^{BE} - 1 = 7$. We replace this uniform random variable with a geometric random variable with parameter p_1^n (see Approximation 4). Therefore the distribution of the number of slots X_1 that the node spends in BO_1 is $P[X_1 = k] = (1 - p_1^n)^k p_1^n$ for $k = 0, 1, \cdots \infty$. Choosing $p_1^n = 1/4.5$ would cause the geometric distribution to have the same 'mean' number of backoff slots as the uniform distribution, which is equal to 3.5.

On leaving BO_1, the node moves to the CS_{11} state, which corresponds to the first of the two slots a node has to confirm that the channel is idle. If the channel is found to be idle in the first slot, which occurs with probability p_i^c, the node moves to the state CS_{12} at the next slot[3]. The notation CS_{12} denotes the second slot corresponding to the first backoff stage, BO_1. In general, we adopt the notation CS_{ij}, $1 \leq i \leq 5$, $1 \leq j \leq 2$, to denote the j^{th} carrier sensing slot after the i^{th} random backoff stage, BO_i. If the node again finds the channel to be idle, it enters the *transmit* (TX) state and starts transmitting the packet. Note that the probability of finding the channel idle in the second slot does not equal p_i^c since the channel state is *not* independent between slots (see Approximation 2). We characterize the probability that the second slot is idle by the conditional probability $p_{i|i}^c$, which is the probability that the channel is idle in the second slot given that it is idle in the first slot. When the node is in the TX state, it spends N slots in that state (since the length of a packet, in terms of number of slots, is equal to N) and then transitions to the IDLE state with probability 1.

On the other hand, if the channel had been found busy when the node was in CS_{11} or CS_{12} states, which happens with probabilities $(1 - p_i^c)$ and $(1 - p_{i|i}^c)$ respectively, the node transitions to the second backoff stage BO_2. The number of slots X_2 that the node spends in BO_2 is again geometrically distributed with parameter $p_2^n = 1/8.5$, since BE=4 for BO_2: $P[X_2 = k] = (1 - p_2^n)^k p_2^n$ for $k = 0, 1, \cdots \infty$.

Following similar arguments, a complete Markov chain can be constructed starting from the IDLE state till either the packet has been successfully transmitted or the maximum number of allowed random backoff stages (equal to 5 as per the IEEE 802.15.4 standard) has been reached. The full chain is depicted in Fig. 2, where $p_3^n = p_4^n = p_5^n = 1/16.5$ since BE=5 for $\text{BO}_i : i = 3, 4, 5$. The node transitions to IDLE state from CS_{51} or CS_{52} if the channel is found busy, indicating an access failure.

The steady state occupancy can be obtained by solving the Markov chain, whose steady state equations are shown in Appendix A. The probability $p_{i|i}^c$ that the channel is idle at the next slot given that it is idle at the current slot, can be computed by noting that:

$$p_i^c = p_{i|i}^c \, p_i^c + p_{i|b}^c (1 - p_i^c) \tag{2}$$

where $p_{i|b}^c$ is the probability that the channel is idle at the next slot given that it is busy at the current slot and is equal to $1/N$, where N is the length of the packet in terms of number of slots. Rewriting (2) and using $p_{i|b}^c = 1/N$, we have:

$$p_{i|i}^c = \frac{p_i^c - p_{i|b}^c (1 - p_i^c)}{p_i^c} = \frac{N p_i^c - 1 + p_i^c}{N p_i^c} \tag{3}$$

[3] As per Approximation 2, p_i^c is the long-term probability that the channel is idle.

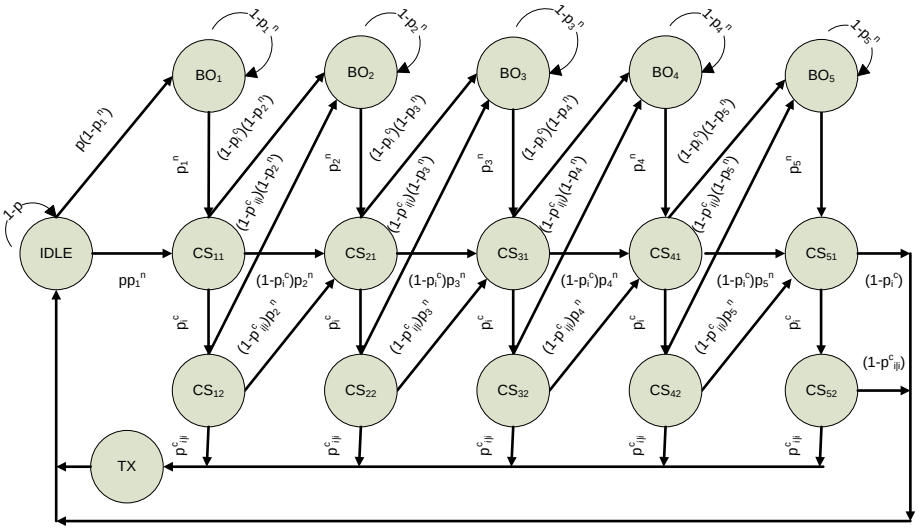

Figure 2: Embedded Markov chain model for an IEEE 802.15.4 sensing node. The notation $\text{BO}_i : 1 \leq i \leq 5$ represents the five random backoff stages and the notation $\text{CS}_{ij} : 1 \leq i \leq 5, 1 \leq j \leq 2$, denotes the j^{th} carrier sense attempt after the i^{th} random backoff stage, BO_i.

We are now in a position to evaluate the probability that any node would begin transmission in a generic slot, p_t^n. By Approximation 3, the probability that a node transmits in a generic slot is equal to the ***steady state*** probability that the node is in one of the states where it is sensing the channel for a second consecutive slot ($i.e.$, $\bigcup_{i=1}^{5} CS_{i2}$) multiplied by $p_{i|i}^c$. Note that $\pi(cs_{i2})$ (see Appendix A for detailed expressions) denotes the steady-state proportion of transitions into state CS_{i2}. To obtain the long-term proportion of time that the chain is in $\bigcup_{i=1}^{5} CS_{i2}$, we need to account for the time spent in each state [20]. Since the dwell time in TX state is N slots and that in all other states is 1 slot, the probability p_t^n is given by:

$$p_t^n = \left(\frac{\sum_{i=1}^{5} \pi(cs_{i2})}{\pi(idle) + N\pi(tx) + \sum_{i=1}^{5}\sum_{j=1}^{2} \pi(cs_{ij}) + \sum_{i=1}^{5} \pi(bo_i)} \right) p_{i|i}^c \tag{4}$$

where $\pi(idle)$, $\pi(tx)$ and $\pi(bo_i)$ are the steady state proportions of transitions into states IDLE, transmit (TX) and the i^{th} backoff stage respectively and the probability $p_{i|i}^c$ is as computed in (3). It may be noted that the denominator of (4) is equal to 1 for $N = 1$.

4.2 Channel state model

Knowing the probability p_t^n that an individual station transmits in a generic slot, we can now develop a Markov chain model for the channel states. Suppose the channel is in the (IDLE,IDLE) state ($i.e.$, idle for two consecutive slots); it continues to remain in that state if none of the nodes begins transmission, which occurs with probability $\alpha = (1 - p_{t|ii}^n)^M$, where M is the number of sensing nodes, excluding the coordinator. The probability that any node begins transmission, given that the channel has been idle for two consecutive slots, is denoted by $p_{t|ii}^n$ and computed as follows:

$$p_{t|ii}^n = \frac{p_t^n}{p_{ii}^c} = \frac{p_t^n}{p_{i|i}^c \, p_i^c} = \frac{N p_t^n}{N p_i^c - 1 + p_i^c} \tag{5}$$

where the last equality in (5) is obtained using the expression for $p_{i|i}^c$ in (3).

On the other hand, when exactly one node begins transmission and others refrain, the channel progresses to the SUCCESS state, which represents a successful transmission. This happens with probability $\beta = M p_{t|ii}^n (1 - p_{t|ii}^n)^{M-1}$. When the channel is in the SUCCESS state, it spends N slots in that state since the length of all packets is assumed to be N slot-durations.

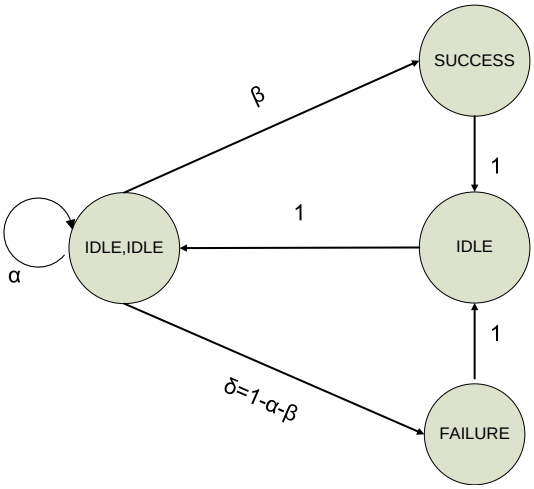

Figure 3: Channel state model. The transition probabilities α and β are given by: $\alpha = (1 - p^n_{t|ii})^M$ and $\beta = Mp^n_{t|ii}(1 - p^n_{t|ii})^{M-1}$, where M is the number of sensing nodes and $p^n_{t|ii}$ is the probability that any node transmits given that the channel was idle in two consecutive slots (5).

The channel goes from the (IDLE,IDLE) state to the FAILURE state if more than one node begins transmission *simultaneously*, which happens with probability $\delta = 1 - \alpha - \beta$. Since there is no collision detect mechanism, the channel remains in the FAILURE state for the entire packet transmission time, or, N slot durations. At the end of the transmission, successful or not, the channel returns to the (IDLE,IDLE) state through an intermediate IDLE state.

The Markov chain for the channel, as shown in Fig. 3, can be solved to determine the probability that the channel remains idle for two consecutive slots, p^c_{ii}:

$$p^c_{ii} = \frac{1}{1 + (N+1)(1-\alpha)} \tag{6}$$

Using (3), the probability that the channel is idle at any generic slot, p^c_i, can be obtained as follows:

$$p^c_i = \frac{p^c_{ii}}{p^c_{i|i}} = \frac{Np^c_{ii} + 1}{N+1} = \frac{2-\alpha}{1 + (N+1)(1-\alpha)} \tag{7}$$

Since p^n_t in (4) is a function of p^c_i through $p^c_{i|i}$ (see eqn. (3)) and p^c_i in (7) is a function of p^n_t through α, we have a consistent system of equations which can be solved numerically.

4.3 Aggregate channel throughput

The aggregate channel throughput S is defined as the fraction of time spent in successful transmissions. This is given by the steady state probability of being in the SUCCESS state in Fig. 3 and can be derived to be:

$$S = \frac{N\beta}{1 + (N+1)(1-\alpha)} = \frac{NMp^n_{t|ii}(1 - p^n_{t|ii})^{M-1}}{1 + N\left(1 - (1 - p^n_{t|ii})^M\right)} \tag{8}$$

where $p^n_{t|ii}$ is as shown in (5) and the parameters α and β are as defined in the caption of Fig. 3. See Appendix B for a derivation of (8).

4.4 Average power consumption per node

In order to determine the average power consumption of a node, we need to identify the various states of a radio and the associated power expenditures, including long-term average dissipation in the various states as well as power consumption during state transitions. For illustrative purposes, we consider the Chipcon 802.15.4-compliant RF transceiver, CC2420 [6]. The Chipcon radio supports the following four states:

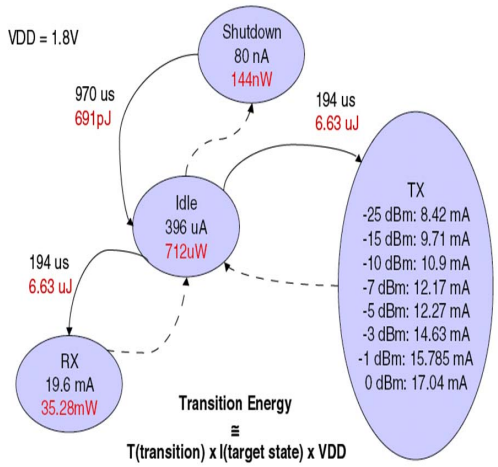

Figure 4: Energy states and transitions for the CC2420 radio. The energy consumption associated with a transition from state S_1 to state S_2 is given by the product of three parameters: (1) transition time, T (transition) (2) current drawn in the target state, I(S_2), and (3) the supply voltage (VDD) = 1.8V.
Reproduced from [1]

1. *Shutdown* or *Sleep*: The crystal oscillator is switched off and the radio is completely disabled waiting for a startup strobe.
2. *Idle*: The crystal oscillator is turned on and the radio is ready to receive commands to switch to *Transmit* or *Receive* state.
3. *Transmit*: The radio is actively transmitting.
4. *Receive*: The radio is actively receiving.

Detailed measurements of the power consumption in each of these states and the state transition times have been reported in [1], and reproduced in Fig. 4 for convenience. It is apparent from the figure that it takes considerable time to switch from one state to another ($e.g.$, close to 1 ms for the *Shutdown-Idle* transition) and this aspect will have a significant effect on the overall energy consumption in wireless sensor networks, particularly those characterized by low transmission duty cycles.

As indicated before, we consider a beacon-enabled network with no inactive part in the superframe in which the nodes can sleep. Since the power consumption in the *Idle* state is several times more than what might be considered reasonable, it is not sufficient to keep the nodes in the *Idle* state when not transmitting or receiving. We must therefore find alternative ways to put the nodes to sleep, even in the active part of the superframe. However, for benchmarking purposes, we start out by leaving the nodes in *Idle* state when not active. Subsequently, in Section 4.6, we allow the nodes to enter the *Shutdown* state when not active and evaluate its impact on the throughput and power consumption.

So far in our analysis, we have neglected the effect of beacon receptions. Since beacons occupy a very small fraction of the time, neglecting their effect on throughput is justified. However, neglecting beacon durations may not be justified for calculating the energy consumption of the nodes. In fact, at sufficiently low traffic rates, energy consumption due to beacon reception may constitute a significant part of the total energy consumed. Consequently, our energy model is as follows.

The radio stays in the *Idle* state until requested to either receive a beacon or perform a clear channel assessment (CCA); at that time, it transitions to the *Receive* state. If beacon reception was requested, the radio returns to the *Idle* state after receiving the beacon. If CCA was requested, after two CCA slots, it either transitions to the *Transmit* state if the channel is found to be idle or back to the *Idle* state if the channel is busy. In other words, the radio is in:

- *Idle* state when it either has no packet to transmit or when it has one and is backing off (corresponding to the IDLE and BO_i states of Fig. 2),

- *Receive* state when it is doing carrier sensing (corresponding to the CS_{ij} states of Fig. 2) or receiving a beacon, and in
- *Transmit* state when it is transmitting.

Let the beacon duration be n_{beacon} slots. The frequency of beacon reception is $f_{beacon} = 1/BI$, where BI is the beacon interval shown in (1). The fraction of time spent is receiving beacons is thus $p^n_{beacon} = n_{beacon}/BI$. We assume that part of the time spent by a node in IDLE state is used to receive the beacons. This is reasonable, particularly at low traffic rates, since the nodes spend most of their time in IDLE state. It may be noted that, in a 1-hop sensor-net, the only time a sensing node is receiving data is during a beacon duration. While it may be possible to explicitly define a node state for this beacon receive duration, we make a simplifying assumption that the beacon reception occurs during the node's IDLE state and adjust the power consumption budget accordingly. This adjustment is necessary since the radio's *Receive* state power expenditure is several orders of magnitude higher than its *Idle* state power dissipation. A similar observation holds for the radio's *Idle*-to-*Receive* transition. We assume that the time required for this transition is budgeted off the node's IDLE state, but that the power consumed during this transition is on the order of the radio's *Receive* state power. The latter assumption may be pessimistic but is necessitated by the fact that no authentic figures are available in the literature for actual power consumption during the *Idle*-to-*Receive* transition. Further, we have assumed that the radio ramp-down times are negligible.

In light of the above discussion, the average power expenditure of any node, Y_{av}, can be expressed as follows:

$$Y_{av} = (p^n_i - p^n_{beacon} + p^n_{bo} - p^n_{ir})Y_{Idle} + (p^n_{cs} + p^n_{ir} + p^n_{beacon})Y_{rx} + p^n_{tx}Y_{tx} \tag{9}$$

where Y_{Idle}, Y_{rx} and Y_{tx} are the power expenditures corresponding to the radio's *Idle*, *Receive* and *Transmit* states respectively. The parameter p^n_{ir} denotes the *fraction of time* spent in switching the radio from *Idle* to *Receive* state. This transition happens whenever the backoff counter reads 1 and once every beacon interval (BI) for beacon reception. In each of these occasions, the radio spends 192 μs, or equivalently, 0.6 backoff slots[4]. Finally, the parameters p^n_i, p^n_{bo}, p^n_{cs} and p^n_{tx} denote the *fractions of time* spent by a node in IDLE, backoff (any BO_i), carrier sense (any CS_{ij}) and transmit (TX) states respectively of Fig. 2 and are given by:

$$\begin{aligned} p^n_i &= \frac{\pi(idle)}{1-\pi(tx)+N\pi(tx)} \\ p^n_{bo} &= \frac{\sum_{i=1}^{5}\pi(bo_i)}{1-\pi(tx)+N\pi(tx)} \\ p^n_{cs} &= \frac{\sum_{i=1}^{5}\sum_{j=1}^{2}\pi(cs_{ij})}{1-\pi(tx)+N\pi(tx)} \\ p^n_{tx} &= \frac{N\pi(tx)}{1-\pi(tx)+N\pi(tx)} \end{aligned} \tag{10}$$

Note that the denominator of all equations in (10) should strictly be:

$$\pi(idle) + \sum_{i=1}^{5}\pi(bo_i) + \sum_{i=1}^{5}\sum_{j=1}^{2}\pi(cs_{ij}) + N\pi(tx) \tag{11}$$

since any node spends N slots when in the transmit state and 1 slot in all other states. However, $\pi(idle)+\sum_{i=1}^{5}\pi(bo_i)+\sum_{i=1}^{5}\sum_{j=1}^{2}\pi(cs_{ij})+\pi(tx) = 1$, and therefore equation (11) can be simplified to $1-\pi(tx)+N\pi(tx)$, as shown in (10).

4.5 Performance metric: per node bytes-per-Joule capacity

A metric that combines per-node throughput and energy consumption, is the per-byte energy cost [26], or its inverse, the bytes-per-Joule capacity [19]. We use a normalized version of the latter (denoted by η) which is defined as follows:

$$\eta = \frac{(S/M) \times \left(250 \times 10^3/8\right)}{Y_{av}} \tag{12}$$

[4]Recall that the duration of each backoff slot as per IEEE 802.15.4 standard is 320 μs.

Table 1: Throughput, per-node power consumption and bytes-per-Joule capacity *without shutdown*, as a function of traffic rate λ. The number of sensing nodes, M, is equal to 12 and the length of a packet, N, in terms of number of slots, is equal to 10.

λ	0.002	0.004	0.006	0.008	0.01	0.02	0.03	0.04
S	0.024	0.048	0.071	0.094	0.118	0.228	0.327	0.408
Y_{av} (mW)	0.82	0.90	0.98	1.05	1.13	1.53	1.93	2.21
η (KB/J)	73	132	181	222	257	370	421	438

λ	0.05	0.06	0.07	0.08	0.09	0.1	0.2	0.4	0.8
S	0.468	0.510	0.538	0.556	0.569	0.577	0.585	0.556	0.523
Y_{av} (mW)	2.66	2.97	3.24	3.48	3.69	3.88	5.14	6.01	6.94
η(KB/J)	437	426	412	397	383	369	283	226	191

where S is the overall throughput (8) and M is the number of sensing nodes. The throughput seen by each user is therefore S/M (by symmetry). The factor $(250 \times 10^3/8)$ is due to the fact that the channel capacity is 250 Kbps in the 2.4 GHz ISM band, or equivalently, $(250 \times 10^3/8)$ bytes/sec.

Table 1 shows the throughput (8), average power consumption (9) and bytes-per-Joule capacity (12) as a function of traffic rate λ, for beacon order $BCO = 6$ ($\Rightarrow p^n_{beacon} = 1/3072$), $n_{beacon} = 2$, $M = 12$ and $N = 10$. The parameter λ in Table 1 is in units of number of packets per packet duration, or equivalently, $(250 \times 10^3 \times \lambda)$ bps since the channel capacity is 250 Kbps. Without shutting down the nodes, we note that the average power consumption is on the order of 1 mW for low packet arrival rates. In the next section, we show how the power consumption can be brought down by an order of magnitude by shutting down the radios when a node is inactive.

4.6 Shutting down the radio between transmissions

We now consider the case when radios are allowed to enter the *Shutdown* state if there is no packet to be transmitted. The energy model in this case is as follows.

If there is no packet waiting to be transmitted, $i.e.$, when the node is in the IDLE state of Fig. 2, the node remains in its *Shutdown* state. Whenever a new packet arrives for transmission, the radio is woken up to perform carrier sensing and subsequent transmission. It is seen from Fig. 4 that it takes about 3 slots (960 μs) to switch the radio from the *Shutdown* state to the *Idle* state and another six-tenths of a slot (192 μs) to switch to the *Receive* slate. The total time from radio *Shutdown* to *Receive* state is therefore 3.6 slots. We claim that this transition time does not affect the throughput or latency significantly, but results in considerable energy savings. This is because the standard requires that every node back off for a random number of slots (between 0 and 7) before sensing the channel for the first time and this backoff time can be used to turn on the radio. Depending on the exact number of backoff slots, additional slots may or may not be needed to completely account for radio start-up time. The increase in the average number of slots that a node has to wait before the first carrier sensing attempt can be accounted for by using a different p^n_1 (the parameter that determines the average number of slots spent in BO_1 state) in the analysis, without altering the results significantly. If the radio start-up time is 3.6 slots (as is the case for Chipcon CC2420 radio), the distribution of the random variable dictating the number of backoff slots corresponding to the first random backoff stage is given by the distribution of $\max(x, 3.6)$, where $x \sim U(0, 7)$ denotes an uniformly distributed random variable in the range $[0, 7]$. We approximate the distribution of the random variable $\max(x, 3.6)$ by a geometric distribution and set the parameter $p^n_1 = 1/5.55$. This ensures that the mean of the geometric distribution is equal to the mean of the distribution of $\max(x, 3.6)$, which can be shown to be equal to 4.55.

A time diagram showing the radio state transitions is shown in Fig. 5. The expression for average power consumed in this case is:

$$\begin{aligned} Y_{av} &= (p^n_i - p^n_{beacon} - p^n_{si})Y_{shut} + (p^n_{bo} - p^n_{ir} + p^n_{si})Y_{Idle} \\ &\quad +(p^n_{cs} + p^n_{ir} + p^n_{beacon})Y_{rx} + p^n_{tx}Y_{tx} \end{aligned} \tag{13}$$

where Y_{shut} is the power consumed in the *Shutdown* state (due to leakage) and p_{si} is the *fraction of time* spent by a radio in the transition from *Shutdown* to *Idle* state before beacon reception. Comparing (13) with (9), we can see that the coefficients associated with Y_{tx} and Y_{rx} are identical. The only differences are in the coefficients of Y_{idle} and the newly defined Y_{shut}, which represent the *Idle* state and *Shutdown* state power consumptions respectively. These

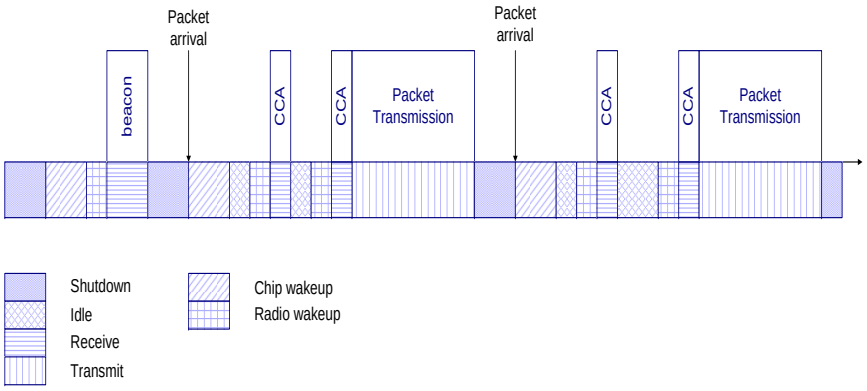

Figure 5: Time diagram showing energy state transitions of a IEEE 802.15.4 radio when nodes are allowed to sleep between transmissions. Note that, when nodes are allowed to sleep between transmissions, each beacon reception interval is preceded by a chip wake-up interval (radio transitions from *Shutdown*-to-*Idle*) and a radio wake-up interval (radio transitions from *Idle*-to-*Receive*). From an energy consumption viewpoint, the chip wake-up duration is associated with the radio *Idle* state and the radio wake-up duration is associated with its *Receive* state. Note also that a chip wake-up duration need not be followed immediately by a radio wake-up duration. For example, if a node has chosen to wait 7 slots, it could use 3 slots for chip wake-up, followed by 3.4 slots idle and then 0.6 slot for radio wake-up, before sensing the channel.

Table 2: Throughput, per-node power consumption and bytes-per-Joule capacity *with shutdown*, as a function of traffic rate λ. The number of sensing nodes, M, is equal to 12 and the length of a packet, N, in terms of number of slots, is equal to 10.

λ	0.002	0.004	0.006	0.008	0.01	0.02	0.03	0.04
S	0.024	0.048	0.071	0.094	0.117	0.228	0.327	0.407
Y_{av} (mW)	0.11	0.19	0.27	0.36	0.44	0.86	1.28	1.68
η (KB/J)	539	630	659	673	680	677	651	616

λ	0.05	0.06	0.07	0.08	0.09	0.1	0.2	0.4	0.8
S	0.467	0.509	0.537	0.556	0.568	0.577	0.585	0.556	0.525
Y_{av} (mW)	2.05	2.39	2.68	2.94	3.18	3.39	4.78	6.02	6.95
η (KB/J)	578	542	509	480	455	433	311	235	192

differences are discussed below:

- Since the radio is shut down during node idle times corresponding to IDLE state of Fig. 2 (represented by the parameter p_i^n), the associated power expenditure is Y_{shut}, as opposed to Y_{idle} in (9).
- We have made the simplistic assumption that the fraction of time spent in receiving beacons, p_{beacon}^n, is budgeted off the radio's *Shutdown* state. Note that, this time was taken off the *Idle* state in (9).
- We have assumed that the *Shutdown*-to-*Idle* transition time (approximately 3 slots for Chipcon CC2420 radio), "preceding a beacon reception", is taken off the radio's *Shutdown* state. Since the beacon frequency is f_{beacon}, the proportion of time spent in this transition mode is given by $3f_{beacon}$. In absence of any authentic data, we have assumed that the corresponding power expenditure is equal to Y_{idle} (which, again, may be pessimistic).
- It may be noted that the *Shutdown*-to-*Idle* transition time "preceding a data transmission" need not be accounted for separately since its effect has already been considered in the modified p_1^n discussed at the beginning of this section.

Table 2 shows the throughput, average power consumption and bytes-per-Joule capacity with radio shutdown, as a function of traffic rate λ. All parameters are the same as discussed in Section 4.5 for the 'without shutdown' case.

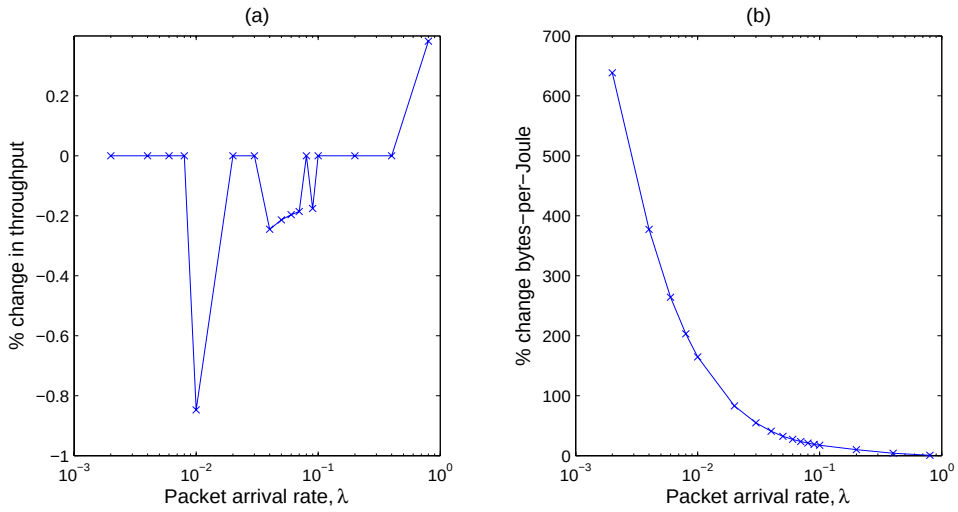

Figure 6: Illustrating the percentage change in throughput (a) and bytes-per-Joule capacity (b) when radios are allowed to shut down, compared to 'no shutdown'. It is clear from the figure that the change in throughput is within $\pm 1\%$ for all values of λ. However, the improvement in bytes-per-Joule capacity is dramatic for smaller values of λ. This improvement can be attributed to a significant reduction in the average power consumption when radios are allowed to shut down between transitions.

At very low traffic rates, the nodes spend most of their time waiting for packets to arrive. Shutting down the radio during these wait times reduces the power expenditure considerably, as is evident from comparing Tables 1 and 2 for low values of λ. For higher values of λ, the amount of time spent in *Shutdown* state is small and hence shutting down the radios at these times does not reduce the average power consumption significantly. In fact, at high enough traffic rates (for $\lambda \geq 0.4$ in the tables), shutting down the radios between transmissions may be costlier than just leaving them in their idle states due to the transition overhead (additional slots required to account for radio startup and associated energy expenditure) involved.

It is also apparent from Table 2 that there is no significant change in throughput due to shutting down the radio between transmissions. For easy comparison, we have shown the percent change in throughput for the 'with shutdown' case, with respect to the 'without shutdown' case, in Fig. 6(a). As can be seen from the figure, the change in throughput is within $\pm 1\%$ for all values of λ. Intuitively, the reason why the throughput does not change significantly is that, a major part of the delay incurred due to the transition from *Shutdown* to *Idle* state is present even in the 'no shutdown' case, in the form of initial random backoff delay. Consequently, the transition delay does not introduce too much of an overhead. An interesting behavior that can be observed from the tables is that, at high packet arrival rates, shutting down the radio actually improves the throughput, albeit marginally. This is due to the typically higher number of slots (to account for radio start-up time) that each node has to wait before sensing the channel, which is equivalent to having a longer backoff and thereby, better contention resolution. Consequently, shutting down the radio when there are no packets to transmit yields higher bytes-per-Joule capacity at all traffic rates (see Fig. 6(b)).

As indicated before, the results shown in Table 2 are for a 12-node sensor network, assuming a packet length equal to 10 slots. Shorter packet lengths and larger number of sensors, both characteristics of typical sensor networks, would cause the average power consumption to increase due to increased transition overhead and increased contention respectively. For $\lambda = 0.002$, simulation results suggest that 17% of the power consumed is due to contention resolution (carrier sensing *etc*.). For $\lambda = 0.02$, this quantity goes up to 25%. It is clear, therefore, that the contention mechanism causes significant overhead and more needs to be done if the average power consumption is to reduced to around 100 μW. Interestingly, it is suggested in [21] that "environmental scavenging" may be a potent way for meeting the energy requirements of sensor networks if the average power expenditure per node is on the order of 100 μW. One way to reduce the contention overhead and thereby, the average power consumption, would be to initialize the Contention Window (CW) to 1 instead of 2 as currently specified in the standard. In the next section, we analyze the performance of the 802.15.4 MAC with this modification. While our proposed modification does not quite achieve the power consumption goal advocated in [21], it does provide a significant improvement in throughput and bytes-per-Joule

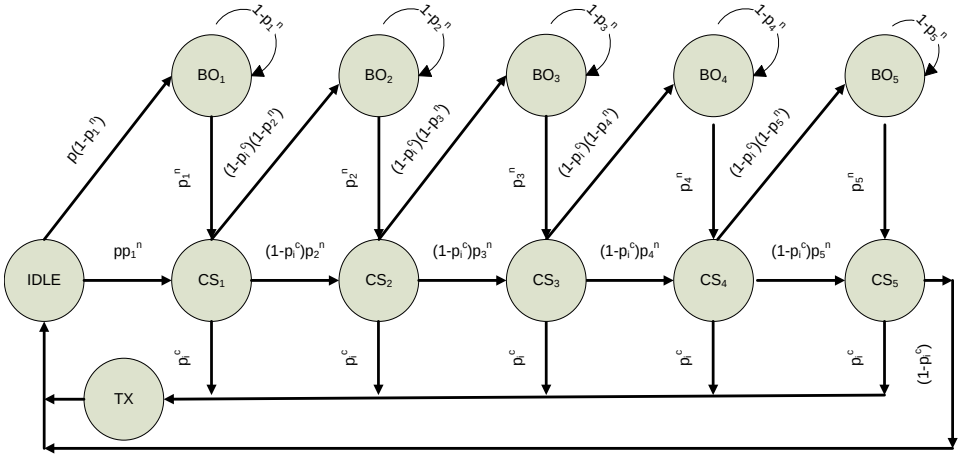

Figure 7: Markov chain model for an IEEE 802.15.4 sensor node with CW=1.

capacity over the standard, particularly at higher packet arrival rates.

5 Proposed modification: Initialization of CW with 1

The IEEE 802.15.4 standard specifies that the length of the contention window, CW, be initialized to 2. This forces the nodes to ensure that the channel is idle for two consecutive slots before it can begin to transmit. The reason for setting CW=2 initially is to eliminate the possibility of collision with an ACK frame. ACK frames are transmitted without backoff or contention, a 'turnaround time'[5] duration after the corresponding data frame. Any node sensing the idle time between a data frame and an ACK frame could mistakenly interpret the channel as being idle and, if CW was initialized to 1, could begin transmission at the next slot, thereby colliding with the ACK frame. The 802.15.4 standard attempts to avoid this collision possibility by specifying an initial contention window of length 2 slots [4].

However, there are several applications where there is no real need for MAC-level acknowledgements. A large number of sensors that observe the same phenomena can provide the necessary redundancy in coverage; since coordinators are typically provided with data aggregation capabilities, redundancy in sensor deployment could obviate the need for individual acknowledgements. In such applications, initializing CW to 2 may not provide any better collision resolution. On the other hand, significant improvements in throughput and energy efficiency can be realized by using a contention window of length 1. In this section, we analyze the performance of the standard with this proposed modification. Our analysis is based on the same set of approximations discussed in Section 4.

5.1 Node state model

The behavior of an individual node can be represented by means of an embedded Markov chain in a manner similar to that in Section4.1. The only difference is that, instead of having two carrier sense states after every backoff, there would just be one now. Specifically, from state BO_i, the node moves to CS_i with probability p_i^n. From CS_i, it either goes to the TX state if the channel is found idle (which occurs with probability p_i^c) or to the next backoff stage if the channel is busy (which occurs with probability $(1 - p_i^c)$). The Markov chain for a 802.15.4 node with CW=1 is shown in Fig 7. Its steady state probabilities can be obtained by solving the state balance equations of the Markov chain, as shown in Appendix C.

As in Section 4.1, the probability that a node starts transmission in any generic slot, or equivalently, the steady-state probability that a node transmits (by Approximation 3), can be shown to by:

$$p_t^n = p_{cs}^n \, p_i^c = \left(\frac{\sum_{i=1}^{5} \pi(cs_i)}{\pi(idle) + N\pi(tx) + \sum_{i=1}^{5} [\pi(cs_i) + \pi(bo_i)]} \right) p_i^c \tag{14}$$

[5]The IEEE 802.15.4 standard define a *turnaround time* as the time required by a radio to switch from transmit to receive mode and *vice versa*. It is the same as the radio start-up time (192 μs).

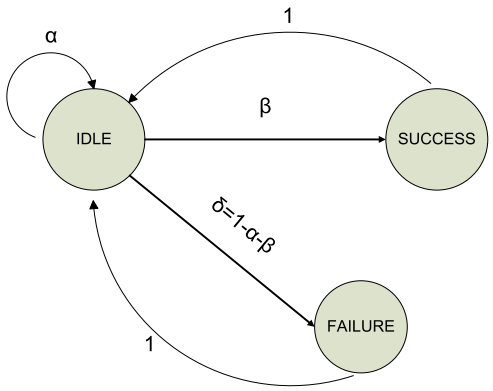

Figure 8: Channel state model with CW=1. The transition probabilities α and β are given by: $\alpha = (1 - p^n_{t|i})^M$ and $\beta = Mp^n_{t|i}(1 - p^n_{t|i})^{M-1}$, where M is the number of sensing nodes and $p^n_{t|i}$ is the probability that any node transmits given that the channel was idle in the previous slot, which is simply the probability that the node sensed the channel in that slot, p^n_{cs} (see eqn. 14).

Note that the probability $p^c_{i|i}$ in (4) has been replaced by p^c_i in (14) as a consequence of our proposed CW=1 modification.

5.2 Channel state model

Given our approximation that the channel sees a probability p^n_t that any node transmits in a generic slot (see Approximation 3 in Section 4), the channel behavior can be represented by means of a Markov chain. For CW=1, channel state transitions are as follows.

The channel is in IDLE state when there is no ongoing transmission. It continues to remain in the IDLE state at the next slot if no node attempts a transmission. This happens with probability $\alpha = (1 - p^n_{t|i})^M$, where $p^n_{t|i}$ is the probability that a node begins transmission in any generic slot, given that the channel was idle in the previous slot, and is simply equal to the probability that a node sensed the channel in that slot, p^n_{cs} (see eqn. 14). On the other hand, if one node starts transmission and others refrain, which happens with probability $\beta = Mp^n_{t|i}(1 - p^n_{t|i})^{M-1}$, the channel transitions to the SUCCESS state. With probability $\delta = 1 - \alpha - \beta$ that more than one node start to transmit at the same time, the channel goes to the FAILURE state, indicating an unsuccessful transmission. It spends N slots each in the SUCCESS and FAILURE states and then returns to the IDLE state with probability 1. The channel state diagram for CW=1 is shown in Fig. 8. The probability that the channel is idle, p^c_i, can be derived to be:

$$p^c_i = \frac{1}{1 + N(1 - \alpha)} = \frac{1}{1 + N(1 - (1 - p^n_{t|i})^M)} \tag{15}$$

Since $p^n_{t|i}$ is a function of p^c_i and p^c_i in is a function of $p^n_{t|i}$ (15), we have a consistent set of equations which can be solved numerically.

5.3 Aggregate channel throughput

The aggregate channel throughput can be derived from the Markov chain of Fig. 7 and is given y:

$$S = \frac{N\beta}{1 + N(1 - \alpha)} = \frac{NMp^n_{t|i}(1 - p^n_{t|i})^{M-1}}{1 + N\left(1 - (1 - p^n_{t|i})^M\right)} \tag{16}$$

The proof is similar to that shown in Appendix B for CW=2 and is omitted.

Table 3: Throughput, per-node power consumption and bytes-per-Joule capacity *with shutdown*, as a function of traffic rate λ, for CW=1. The number of sensing nodes, M, is equal to 12 and the length of a packet, N, is equal to 10 slots.

λ	0.002	0.004	0.006	0.008	0.01	0.02	0.03	0.04
S	0.024	0.048	0.071	0.099	0.117	0.228	0.327	0.407
Y_{avg} (mW)	0.1	0.18	0.25	0.33	0.40	0.78	1.16	1.54
η (KB/J)	588	678	711	727	734	730	703	668

λ	0.05	0.06	0.07	0.08	0.09	0.1	0.2	0.4	0.8
S	0.469	0.518	0.552	0.577	0.595	0.608	0.634	0.591	0.583
Y_{avg} (mW)	1.89	2.22	2.51	2.77	3.01	3.23	4.64	6.12	6.86
η (KB/J)	630	593	559	529	502	479	347	263	216

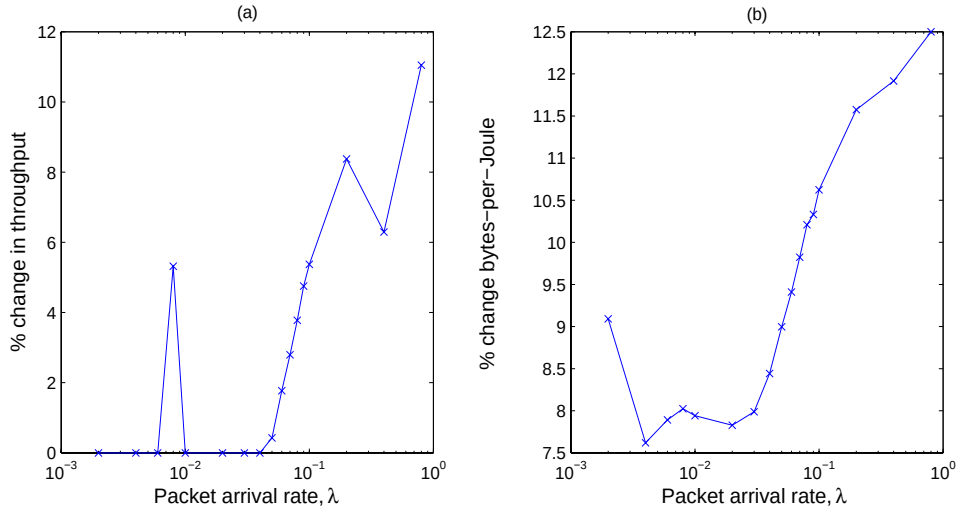

Figure 9: Illustrating the percentage change in (a) throughput and (b) bytes-per-Joule capacity for CW=1 compared to CW=2, when radios are allowed to shut down.

5.4 Average power consumption per node

The average power consumption per node when the radio is shutdown between transmissions is identical to (13), except that p_{cs}^n, the *fraction of time* spent by a node channel sensing, is now given by:

$$p_{cs}^n = \frac{\sum_i \pi(cs_{i1})}{1 - \pi(tx) + N\pi(tx)} \tag{17}$$

Table 3 shows the aggregate throughput, the average power consumption per node and the bytes-per-Joule capacity for a 12-node sensor network when CW is initialized to 1. All other parameters are the same as those used in Table 2. Comparing Tables 2 and 3, it is clear that initializing CW with 1 results in about 10% reduction in average power consumption over $CW = 2$ at low traffic rates. This reduction is achieved by trimming the energy consumption due to the contention process. For $\lambda = 0.002$, 11% of the total energy is due to the contention procedure when CW=1, compared to 17% when CW=2. For $\lambda = 0.02$, it is 22% for CW=1 and 25% for CW=2. As far as throughput is concerned, at low traffic rates, there is not much to be gained by initializing CW with 1 compared to CW=2 since the channel would be mostly idle in either case. At higher traffic rates, however, there is a significant improvement in throughput - up to 10%, as is evident from Fig. 9(a). This is because a shorter contention window does a better job of packing the channel with traffic when MAC level acknowledgements are not used. The increased energy efficiency at low data rates and increased throughput at high data rates together produce a bytes-per-Joule capacity that is 10-15% better when CW=1, as can be seen from Fig. 9(b).

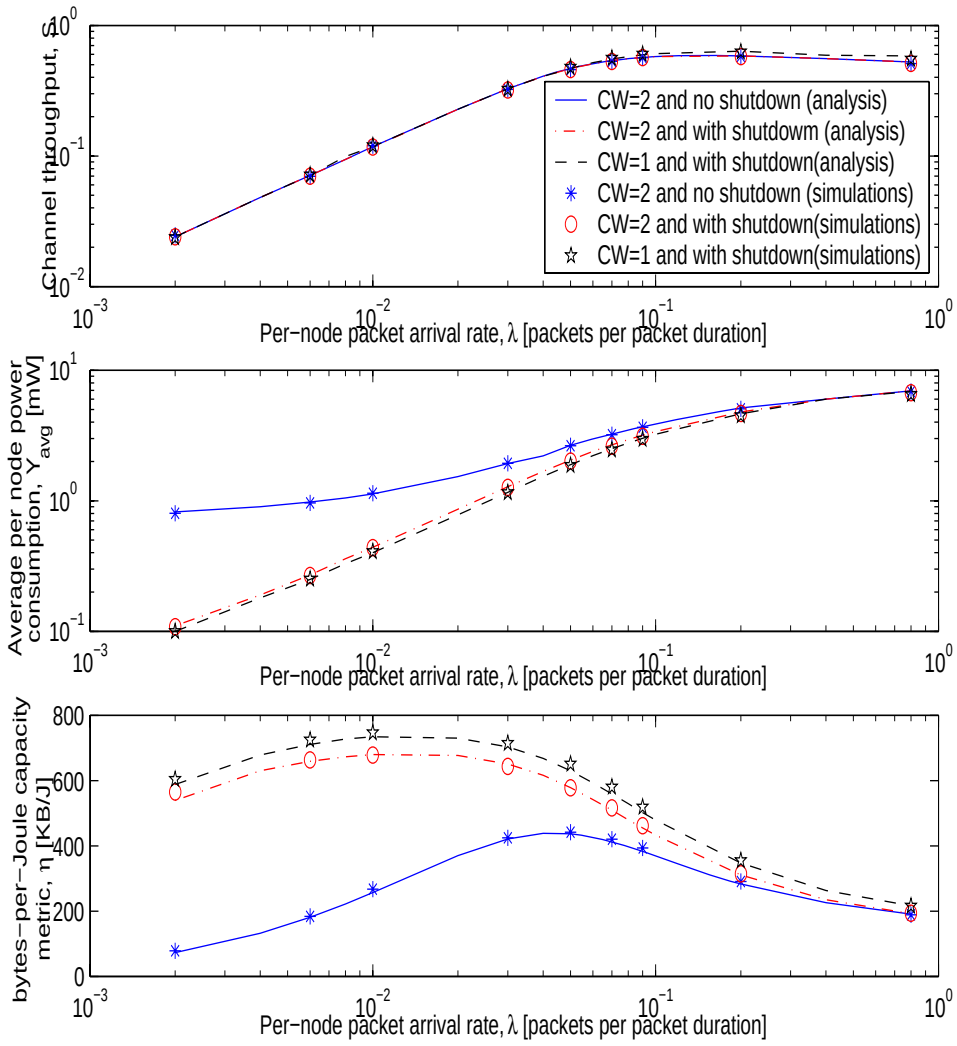

Figure 10: From top to bottom: (a) Channel throughput, S, (b) average power consumption, Y_{avg} (mW) and (c) bytes-per-Joule capacity, η, as a function of the packet arrival rate, λ. Number of sensing nodes, M is 12 and packet length N is 10 slots.

6 Simulations and Discussion

We have verified our analytical modeling by extensive *ns*-2 simulations for different model parameters like the traffic rate (λ) and packet length, N. The simulations are based on the set of assumptions described in Section 3. However, it is important to note that the approximations described in Section 4 were only meant to simplify the analysis and have not been used in the simulations. In fact, the results in this section also serve to verify their validity.

Our simulation used the base 802.15.4 *ns*-2 module developed in [28]. Although their *ns*-2 code is comprehensive in all other aspects, radio shut down has not been included as an option. Furthermore, the energy models available in *ns*-2 are rudimentary and do not support power accounting in the sleep state or the transition times between different states. We have upgraded the code to account for radio shutdown and developed and integrated our own energy model within the existing 802.15.4 module [6].

For our first set of simulations, we used $M = 12$ sensing nodes, each generating packets of length $N = 10$ slots based on a Poisson arrival rate of λ packets per packet duration. A beacon order (BCO) of 6, corresponding to a beacon interval (BI) of 3072 slots (0.983 seconds), and a beacon length of 2 slots were used. Fig. 10 plots the

[6]The modified *ns*-2 modules will be available on request from the authors.

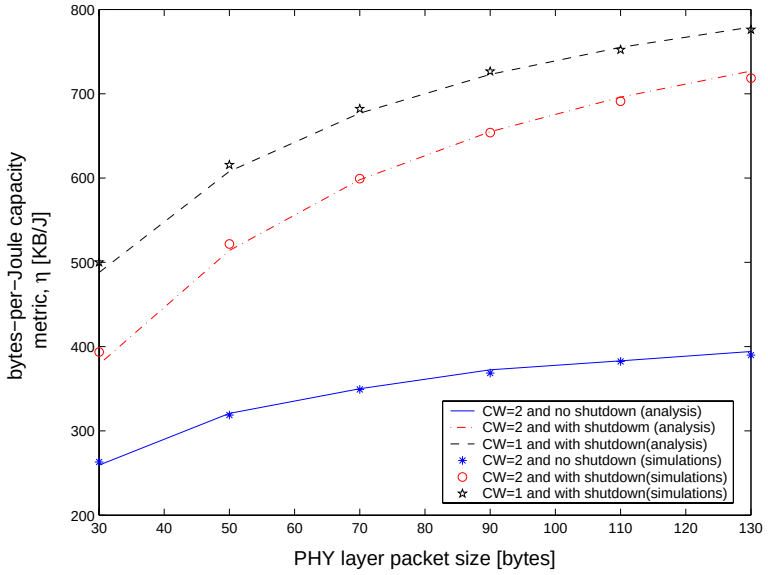

Figure 11: bytes-per-Joule capacity, η, as a function of packet length. Number of sensing nodes, M is 12 and $\lambda = 0.02$

channel throughput (S), average per-node power consumption (Y_{av}) and the bytes-per-Joule metric (η), as functions of λ. The first observation from the plot concerns the accuracy of the analysis. It is evident that our model assumptions and approximations are extremely accurate for all values of packet arrival rates considered. Specifically, this justifies the key analytical model assumptions, namely (a) beacon boundaries have negligible impact on the behavior of the 802.15.4 specification and (b) non-persistent CSMA, with backoff durations chosen from a geometric distribution provides a very accurate model.

Shutting down the nodes between transmissions is a very effective means of reducing the average power consumption, particularly at low packet arrival rates. For the value of N considered, $\lambda = 0.002$ corresponds to an average data rate of 500 bps. At this rate, shutting down the radio provides an eight-fold drop in the average power consumption. However, there is no significant reduction in throughput since the standard-specified initial backoff delay virtually offsets the delay associated with the shutdown to active state transition of the radio. As the arrival rate increases, the benefit of radio shutdown reduces for the obvious reason that the radio spends less and less time in the *Shutdown* state. In fact, it can be seen from Fig. 10 that beyond a high enough arrival rate (λ=0.4 for the parameters chosen), it is no longer advantageous from an energy consumption perspective to shutdown the radio between transmissions.

Reducing the contention window size to CW=1 from the standard-specified CW = 2 does not significantly affect the channel throughput at low packet arrival rates since the channel remains mostly idle in either case. However, as the arrival rate increases, the throughput advantage of CW=1 becomes clear. Intuitively, the reason for this improvement is that a contention window of length 1 reduces the idle time for each node and does a better job of packing the channel with data transmissions. Additionally, the average power consumption for CW=1 is lower than for CW=2, since each node gets a little more sleep time in the former case. The increase in throughput and reduction in power consumption together result in an improvement of between 10% and 15% for the bytes-per-Joule metric, η. Further improvements can be realized by using shorter packet lengths, as discussed next.

In Fig. 11, we have plotted the metric η as a function of the physical (PHY) layer packet length. The number of sensing nodes is $M = 12$ and $\lambda = 0.02$ (equivalent to 5 Kbps). It is clear from the figure that the bytes-per-Joule capacity increases with packet length. Increasing the packet length beyond what is shown in the figure would result in further improvement, but the 802.15.4 standard allows for a maximum PHY payload size of 127 bytes, which, after accounting for the PHY-layer preamble (6 bytes), translates to a total packet size of 133 bytes. Second, shutting down the radio offers a better performance for longer packet lengths. The reason for this is that, for a given data rate, using shorter packets forces the radio to switch on and off more frequently, thereby expending more energy. It may be noted that, for the maximum allowed packet length, shutting down the radio results in a more than 85% improvement in the bytes-per-Joule capacity for CW=2 ($i.e.$, comparing the red and blue curves). Finally, initializing CW=1 produces a noticeably better performance with shorter packets since the fractional overhead that CW=1 cuts down is more for

shorter packets than for longer packets. As can be seen from Fig. 11, for a packet length of 130 bytes, the performance improvement for CW=1 over CW=2 when radios allowed to shut down ($i.e.$, comparing the black and red curves) is only about 5%, while for 30 byte packets, the improvement is more than 25%.

In summary, our key findings are as follows:

- Non-persistent CSMA with backoff durations chosen from a geometric distribution represents a very accurate model of the behavior of the Contention Access Period of IEEE 802.15.4 MAC as is exemplified by the simulations.
- The radio can be safely shutdown between packet transmissions to realize considerable savings in energy without affecting the channel throughput significantly. This is possible due to the specification of an initial backoff delay in the standard that virtually 'cushions' the effect of the radio start-up delay on throughput.
- Using CW=1 instead of the standard-specified value of 2 reduces the energy consumption and increases the throughput in applications which do not require MAC-level acknowledgements. This modification yields better returns for shorter packets.

7 Conclusions

A comprehensive analysis of non-persistent CSMA with the backoff procedure of IEEE 802.15.4 has been presented and it has been shown that the standard specified MAC can be accurately modeled as non-persistent CSMA. Letting the radio enter a *Shutdown* state between transmissions has been shown to be a very effective means of reducing the average power consumption for a very wide range of traffic rates, when the traffic is predominantly uplink. Initializing the contention window length to 1 has been proposed to improve throughput and reduce energy consumption when MAC level acknowledgements are not used.

Several assumptions have been made to simplify our analysis. Future work will focus on extending the analysis to other pragmatic scenarios. For example, while the assumption that all nodes are within the carrier sense range of each other holds for small-area applications like WBANs and networks of PC peripherals, it may not be true for larger scale applications like sensor assisted industrial control and environmental monitoring. A possible future research direction is to remove this assumption and include the possibility of hidden nodes by assuming a certain geographical distribution of the nodes. Finally, we have assumed that there is no buffering at the MAC layer and that new packets are not accepted from the upper layer when the MAC is attempting transmission of a packet. It would be interesting to see the impact of a finite MAC-level buffer size on the throughput and energy consumption of a 802.15.4 sensing node.

APPENDIX

A Steady state transition equations for the Markov chain of Fig. 2

The steady-state probabilities of the embedded Markov chain of Fig. 2 can be obtained by solving the following balance equations. The notation $\pi(state_i)$ denotes the long-term proportion of transitions into $state_i$.

$$\begin{aligned}
\pi(idle) &= (1-p)\pi(idle) + \pi(tx) + (1-p_i^c)\pi(cs_{51}) + (1-p_{i|i}^c)\pi(cs_{52}) \\
\pi(bo_1) &= (1-p_1^n)\left[p\pi(idle) + \pi(bo_1)\right] \\
\pi(cs_{11}) &= p_1^n\left[p\,\pi(idle) + \pi(bo_1)\right] \\
\pi(cs_{12}) &= p_i^c\,\pi(cs_{11}) \\
\pi(bo_2) &= (1-p_2^n)\left[(1-p_i^c)\pi(cs_{11}) + (1-p_{i|i}^c)\pi(cs_{12}) + \pi(bo_2)\right] \\
\pi(cs_{21}) &= p_2^n\left[(1-p_i^c)\pi(cs_{11}) + (1-p_{i|i}^c)\pi(cs_{12}) + \pi(bo_2)\right] \\
\pi(cs_{22}) &= p_i^c\,\pi(cs_{21}) \\
\pi(bo_3) &= (1-p_3^n)\left[(1-p_i^c)\pi(cs_{21}) + (1-p_{i|i}^c)\pi(cs_{22}) + \pi(bo_3)\right] \\
\pi(cs_{31}) &= p_3^n\left[(1-p_i^c)\pi(cs_{21}) + (1-p_{i|i}^c)\pi(cs_{22}) + \pi(bo_3)\right] \\
\pi(cs_{32}) &= p_i^c\,\pi(cs_{31}) \\
\pi(bo_4) &= (1-p_4^n)\left[(1-p_i^c)\pi(cs_{31}) + (1-p_{i|i}^c)\pi(cs_{32}) + \pi(bo_4)\right] \\
\pi(cs_{41}) &= p_4^n\left[(1-p_i^c)\pi(cs_{31}) + (1-p_{i|i}^c)\pi(cs_{32}) + \pi(bo_4)\right] \\
\pi(cs_{42}) &= p_i^c\,\pi(cs_{41}) \\
\pi(bo_5) &= (1-p_5^n)\left[(1-p_i^c)\pi(cs_{41}) + (1-p_{i|i}^c)\pi(cs_{42}) + \pi(bo_5)\right] \\
\pi(cs_{51}) &= p_5^n\left[(1-p_i^c)\pi(cs_{41}) + (1-p_{i|i}^c)\pi(cs_{42}) + \pi(bo_5)\right] \\
\pi(cs_{52}) &= p_i^c\,\pi(cs_{51})
\end{aligned} \tag{18}$$

$$\pi(idle) + \pi(tx) + \sum_{i=1}^{5}\left[\pi(bo_i) + \pi(cs_{i1}) + \pi(cs_{i2})\right] = 1 \tag{19}$$

B Derivation of the throughput expression (8) in Section 4.3

With respect to the Markov chain in Fig. 3, we first define π_{ii}^c, π_i^c, π_f^c and π_s^c as the long term proportions of transitions into states (IDLE, IDLE), IDLE, FAILURE and SUCCESS respectively. The state balance equations corresponding to the channel Markov chain are:

$$\begin{aligned}
\pi_{ii}^c &= \alpha\,\pi_{ii}^c + \pi_i^c \\
\pi_s^c &= \beta\,\pi_{ii}^c \\
\pi_f^c &= (1-\alpha-\beta)\,\pi_{ii}^c \\
\pi_i^c &= 1 - \pi_{ii}^c - \pi_s^c - \pi_f^c
\end{aligned} \tag{20}$$

which can be solved to obtain:

$$\begin{aligned}
\pi_{ii}^c &= \frac{1}{3-2\alpha} \\
\pi_s^c &= \frac{\beta}{3-2\alpha} \\
\pi_f^c &= \frac{\delta}{3-2\alpha} \\
\pi_i^c &= \frac{1-\alpha}{3-2\alpha}
\end{aligned} \tag{21}$$

The fraction of time spent in each state can be obtained by accounting for the actual time spent in each state. Noting that the chain spends N time slots in the SUCCESS and FAILURE states and 1 slot in each of the other states, the

throughput, which is the fraction of time spent in the SUCCESS state, can be obtained as follows:

$$\begin{aligned} S &= \frac{N\pi_s^c}{\pi_{ii}^c + \pi_i^c + N\pi_s^c + N\pi_f^c} \\ &= \frac{1}{1 + (1-\alpha) + N(\beta+\delta)} \\ &= \frac{N\beta}{1 + (N+1)(1-\alpha)} \end{aligned}$$

C Steady state transition equations for the Markov chain of Fig. 7

The steady-state probabilities of the embedded Markov chain of Fig. 7 can be obtained by solving the following balance equations. The notation $\pi(state_i)$ denotes the long-term proportion of transitions into $state_i$.

$$\begin{aligned} \pi(idle) &= (1-p)\pi(idle) + \pi(tx) + (1-p_i^c)\pi(cs_5) \\ \pi(bo_1) &= p(1-p_1^n)\pi(idle) + (1-p_1^n)\pi(bo_1) \\ \pi(cs_1) &= p\pi_1^n\,\pi(idle) + p_1^n\,\pi(bo_1) \\ \pi(bo_2) &= (1-p_i^c)(1-p_2^n)\pi(cs_1) + (1-p_2^n)\pi(bo_2) \\ \pi(cs_2) &= (1-p_i^c)p_2^n\,\pi(cs_1) + p_2^n\,\pi(bo_2) \\ \pi(bo_3) &= (1-p_i^c)(1-p_3^n)\pi(cs_2) + (1-p_3^n)\pi(bo_3) \\ \pi(cs_3) &= (1-p_i^c)p_3^n\,\pi(cs_2) + p_3^n\,\pi(bo_3) \\ \pi(bo_4) &= (1-p_i^c)(1-p_4^n)\pi(cs_3) + (1-p_4^n)\pi(bo_4) \\ \pi(cs_4) &= (1-p_i^c)p_4^n\,\pi(cs_3) + p_4^n\,\pi(bo_4) \\ \pi(bo_5) &= (1-p_i^c)(1-p_5^n)\pi(cs_4) + (1-p_5^n)\pi(bo_5) \\ \pi(cs_5) &= (1-p_i^c)p_5^n\,\pi(cs_4) + p_5^n\,\pi(bo_5) \end{aligned} \tag{22}$$

$$\pi(idle) + \pi(tx) + \sum_{i=1}^{5}[\pi(bo_i) + \pi(cs_i)] = 1 \tag{23}$$

References

[1] B. Bougard, F. Catthoor, D. Daly, A. Chandrakasan, and W. Dehaene. Energy efficiency of the IEEE 802.15.4 standard in dense wireless microsensor networks: Modeling and improvement perspectives. *IEEE DATE 2005*, pages 196 – 201, March 2005.

[2] R. Bruno, M. Conti, and E. Gregori. Optimization of efficiency and energy consumption in p-persistent CSMA-based wireless LANs. *IEEE Trans. Mobile Computing*, 1:10–31, Jan. - Mar. 2002.

[3] F. Calì, M. Conti, and E. Gregori. Dynamic tuning of the IEEE 802.11 protocol to achieve a theoretical throughput limit. *IEEE/ACM Trans. Networking*, 8, no. 6:785–799, Dec. 2000.

[4] E. Callaway. Motorola Labs; Private Communication.

[5] E. Callaway, P. Gorday, L. Hester, J. Gutierrez, M. Naeve, B. Heile, and V. Bahl. Home networking with IEEE 802.15.4: a developing standard for low-rate wireless personal area networks. *IEEE Comm. Mag.*, 40:70–77, Aug 2002.

[6] 2.4 GHz IEEE 802.15.4/Zigbee-ready RF transceiver. `http://www.chipcon.com/files/CC2420_Data_sheet_1_2.pdf`, 2004.

[7] C. Y. Chong and S. P. Kumar. Sensor networks: Evolution, opportunities and challenges. In *Proc. of the IEEE*, volume 91, pages 1247–1256, August 2003.

[8] Micaz wireless measurement system. `http://www.xbow.com`, 2004.

[9] D. Culler, D. Estrin, and M. Srivastava. Overview of sensor networks. *IEEE Computer*, 37:41–49, August 2004.

[10] M2020 mote datasheet. `http://http://www.dust-inc.com/products/main.shtml`, 2005.

[11] A. El-Hoiydi and J.-D. Decotignie. WiseMAC: an ultra low power MAC protocol for the downlink of infrastructure wireless sensor networks. *ISCC 2004*, 1:244–251, July 2004.

[12] N. Golmie, D. Cypher, and O. Rebala. Performance analysis of low rate wireless technologies for medical applications. *Computer Communications (Elsevier)*, 28:1266–1275, June 2005.

[13] Part 15.4: Wireless medium access control and physical layer specifications for low rate wireless personal area networks. Technical report, ANSI/IEEE Standard 802.15.4, Sept. 2003.

[14] E. Jovanov, A. Milenkovic, C. Otto, and P. de Groen. A wireless body area network of intelligent motion sensors for computer assisted physical rehabilitation. *Journal of Neuroengineering and Rehabilitation*, 2, March 2005.

[15] L. Kleinrock and F. A. Tobagi. Packet switching in radio channels: Part I-carrier sense multiple-access modes and their throughput-delay characteristics. *IEEE Trans. Commun.*, 23:1400–1416, Dec. 1975.

[16] G. Lu, B. Krishnamachari, and C. S. Raghavendra. Performance evaluation of the IEEE 802.15.4 MAC for low-rate low-power wireless networks. *IEEE IPCCC 2004*, pages 701 – 706, April 2004.

[17] J. Polastre, R. Szewczyk, and D. Culler. Telos: Enabling ultra-low power wireless research. *IPSN/SPOTS*, pages 364 – 369, April 2005.

[18] J. M. Rabaey, M. J. Ammer, J. L. da Silva, D. Patel, and S. Roundy. Picoradio supports ad hoc ultra-low power wireless networking. *IEEE Computer*, 33:42–48, July 2000.

[19] V. Rodoplu and T. Meng. Bits-per-joule capacity of energy-limited wireless ad hoc networks. *IEEE Globecom*, 1:17–21, Nov. 2002.

[20] S. M. Ross. *Introduction to Probability Models*. Academic Press, 7 edition, 2000.

[21] S. Roundy, P. Wright, and J. Rabaey. *Energy Scavenging for Wireless Sensor Networks with Special Focus on Vibration*. Kluwer Scademic Publishers, 2004.

[22] E. Shih, S. Cho, F. S. Lee, B. H. Calhoun, and A. P. Chandrakasan. Design considerations for energy-efficient radios in wireless microsensor networks. *The Journal of VLSI Signal Processing-Systems for Signal, Image, and Video Technology*, 37:77–94, May 2004.

[23] H. Takagi and L. Kleinrock. Optimal transmission range for randomly distributed packet radio terminals. *IEEE Trans. on Comm.*, 32, Issue 3:246–257, Mar 1984.

[24] N. F. Timmons and W. G. Scanlon. Analysis of the performance of IEEE 802.15.4 for medical sensor body area networking. *IEEE SECON*, 28:1266–1275, Oct. 2004.

[25] L. Wu and P. Varshney. Performance analysis of CSMA and BTMA protocols in multihop networks (I). Single channel case. *Information Sciences (Elsevier)*, 120:159–177, Nov. 1999.

[26] Wei Ye, J. Heidemann, and D. Estrin. Medium access control with coordinated adaptive sleeping for wireless sensor networks. *IEEE Trans. on Networking*, 12, Issue. 3:493–506, June 2004.

[27] J. Zheng and M. J. Lee. *A Comprehensive Performance Study of* IEEE *802.15.4*. IEEE Press, 2004.

[28] J. Zheng and M. J. Lee. Will IEEE 802.15.4 make ubiquitous networking a reality?: A discussion on a potential low power low bit rate standard. *IEEE Comm. Mag.*, 42:140–146, June 2004.